Equivalent parameter study of the mechanical properties of super carbon nanotubes

Min Wang, Xinming Qiu, Xiong Zhang and Yajun Yin

Department of Engineering Mechanics, Tsinghua University, Beijing 100084,
People's Republic of China

E-mail: qxm@tsinghua.edu.cn

Abstract
Theoretical studies are made for recent attention-getting super carbon
nanotubes. The so-called 'super carbon nanotube' is a self-similar structure
constructed from low-order carbon nanotubes. Based on the Euler beam
theory, the equivalent parameters of super tubes are derived from those of
arm tubes, and verified by finite element simulations. Instead of the Young's
modulus E, a new equivalent modulus $E\beta$ is adopted, where β is the ratio of
thickness to diameter for arm tubes. The advantage of this equivalent
modulus is that the Young's modulus and thickness do not need to be
separated in stiffness calculations. The mechanical properties for composites
made of super tubes and matrix are also discussed.

(Some figures in this article are in colour only in the electronic version)

1. Introduction

Recently, super carbon nanostructures with self-similarities
have been predicted, inspired by experiments on perfect Y-
branched carbon nanotubes (CNTs). Li *et al* [1] and Biró
et al [2] obtained Y-branched junctions with very straight and
uniform CNTs in their experiments, and the angles between
arms were close to 120°. Using geometric conservation
laws, Yin *et al* [3] theoretically proved that the Y-branched
junctions with such perfect symmetric structures satisfied the
equilibrium state with both minimum energy and symmetric
geometry. In construction, the perfect Y-branched junction
is similar to the shape of the sp^2 carbon–carbon bond of
graphite. This similarity evokes the proposal of super graphite
(SG) constructed by repeating perfect Y-junction nanotubes
periodically. Additionally, by rolling up SG, a super carbon
nanotube (ST) could be obtained in the similar way of forming
single-walled carbon nanotubes (SWNTs) [4]. This super tube
composed of SWNTs is completely similar to an SWNT itself;
thus a higher-order super tube could be formed obeying these
self-similar rules.

The super tubes are expected to provide special applica-
tions in nanoelectronics and fibre-reinforced composites. The
application of straight CNTs on nanoropes and reinforced
composites is limited by their size scale and the poor capa-
bility of force transfer due to the weak van der Waals intera-
ction between tubes [5]. However, in the construction of the
super tube and super graphite, relatively shorter SWNTs are ar-
ranged into regular net structure through covalent bonds. Wang
et al [6] reported that the SG structures have great flexibility
and outstanding capability in force transfer. Furthermore, the
size scale of a super nanotube will be greatly increased through
the self-similarity. Therefore, macroscale super tubes gener-
ated by self-similarity might have many potential applications.
Currently, the methods of synthesis of these regular and com-
plex structures are the key remaining and challenging issues.
The controlled fabrication of nanostructures inside the pores of
zeolite and other mesoporous materials, used as templates, is
widely used in the process of producing nanomaterial [7, 8].
Recently, hierarchically branched nanotubes have been made
using porous templates [8], which provide a significant
advance in the realization of super structures.

In this paper, $ST^{(N)}$ denotes a super tube obtained through
N times self-similarity from SWNTs. The electrical properties
of $ST^{(1)}$ were explored by using atomic calculations [4],
and the mechanical properties of $ST^{(1)}$ were examined by
employing a shell model [6]. Wang *et al* [6] indicated that the
SGs were ductile due to their hexagonal honeycomb structures,
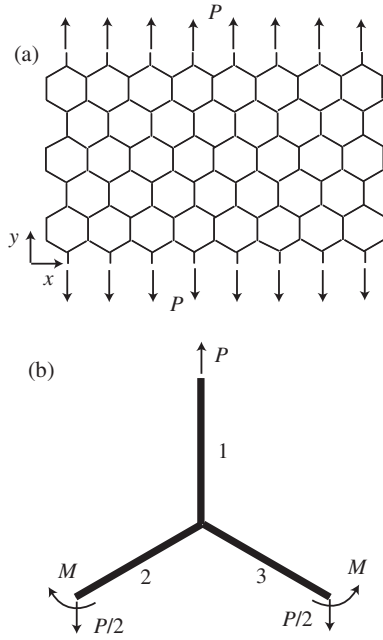
Figure 1. (a) SG with the arms of a lower-order ST, (b) the force diagram of a representative Y-branched junction when the SG is subject to *y*-axis tension.

while the ultimate tensile strength was very high because of the arms' stretching. Pugno [9] evaluated the strength, toughness and stiffness of any order super tubes and fibre-reinforced composites, by using the hierarchical theory. His work was based on the force equilibrium analysis in a special cross section of super tubes.

The geometry parameters, such as arm length and tube diameter, will determine the properties of super tubes. If the equivalent parameters of a lower-order tube are already known, what will be the corresponding parameters of its higher-order tube? In this paper, we are trying to find the relations between the parameters of higher-order super tubes and those of the lower order ones.

2. Model for super graphite and super tube

Li and Chou [10] presented the molecular structural mechanics method, in which the covalent bond between atoms was modelled by a beam with parameters determined through energy equivalence. Here, the beam assumption is used to analyse SG and STs as well. For the super graphite structures as shown in figure 1(a), each arm is a lower-order super tube. The arms are simplified as annular section Euler beams, having rigid connections at the joints. For the small deformation case, this assumption will have acceptable accuracy, especially when the ratio of length to diameter of the arm tube is large. Supposing the mechanical properties and geometry parameters of a lower-order ST are already known, the structural mechanics method could be adopted to analyse the super graphite and super tube structures. By employing solid sectional beams with rigid connections, this method is widely adopted in the analysis of cellular solids used as lightweight structures and energy-absorbing devices [11, 12].

In previous work [6], the mechanics of super structures with arms of SWNTs have been examined using the shell model, which is more appropriate for Y-branched nanotubes. It was indicated that the connection of the Y junction based on SWNTs has different properties from those of the general joint of framework such as a rigid connection or hinge joint. However, during a small deformation, the effect of local deformation at the junction and the change of angle between arms are not very significant, and the changes in atomic level such as bond breaking or recomposing are negligible. Consequently, the beam model is adopted here in the theoretical analysis. It should be noted that the beam model is limited to analysing the mechanical properties of super structures with slender arms in a small deformation.

By self-similarly assembling, the arms of super tubes could be SWNTs or low-order STs. Their equivalent diameter D and equivalent thickness t are defined as $D = (D_o + D_i)/2$ and $t = (D_o - D_i)/2$, where D_o and D_i are the diameters of the outer and inner circles. The wall thickness of the annular section t is small compared with diameter D. Suppose that the equivalent Young's modulus of the arm tube is E, and the arm length is l. On normalizing the length and thickness by the diameter D, two important non-dimensional geometry parameters are defined as

$$\alpha = l/D, \qquad \beta = t/D. \tag{1}$$

Here, the slenderness ratio $\alpha > 5$ for slender beam, while the thickness ratio $\beta \ll 1$ for a thin thickness tube. The cross-section area A, inertia moment I and flexural section modulus W of an annular section beam are given by

$$A = \tfrac{1}{4}\pi(D_o^2 - D_i^2) = \pi D^2 \beta, \tag{2}$$

$$I = \tfrac{1}{64}\pi(D_o^4 - D_i^4) = \tfrac{1}{8}\pi D^4 \beta(1 + \beta^2), \tag{3}$$

$$W = \frac{I}{D_o/2} = \tfrac{1}{4}\pi D^3 \beta(1 - \beta + \beta^2 - \beta^3)(1 - \beta^2). \tag{4}$$

For a thin cylinder, β is small, so the effect of β^2 and its higher orders can be neglected. Hence, equations (2)–(4) can be approximated as

$$A = \pi D^2 \beta, \tag{5}$$

$$I = \tfrac{1}{8}\pi D^4 \beta, \tag{6}$$

$$W = \tfrac{1}{4}\pi D^3 \beta(1 - \beta). \tag{7}$$

3. Super structures subject to uniform tension

3.1. The stress of a Y junction under tension

If a piece of super graphite structure is wide enough, the deformation of each Y-branched junction is the same under uniaxial tension. The reaction force of a representative Y-branched junction under *y*-axis tension is analysed as displayed in figure 1(b). The reaction forces at the three ends are obtained through equilibrium analysis. Under the uniaxial loading in the *y*-direction, arm 1 bears tension only. The uniform stress is

$$\sigma_1 = \frac{F}{A} = \frac{P}{\pi D^2 \beta}. \tag{8}$$

Under the equilibrium condition, the bending moment at the ends of arms 2 and 3 is $M = \sqrt{3}Pl/8$. Arms 2 and 3 bear both tension and bending, thus the arms will have maximum stress at the junction due to the summation of tension and bending:

$$\sigma_2 = \frac{F}{A} + \frac{M}{W} = \frac{P}{\pi D^2 \beta}\left[\frac{1}{4} + \frac{\sqrt{3}\alpha}{2(1-\beta)}\right]. \quad (9)$$

For a slender beam, $\alpha > 5$ and $0 < \beta < 1$, it is clear that $\frac{1}{4} + \frac{\sqrt{3}\alpha}{2(1-\beta)} > 1$. Comparing equation (9) with (8), we have $\sigma_2 > \sigma_1$, which means that under uniaxial tension the maximum stress of super graphite locates right at the Y junction, and is the combination of bending and tension. From magnitude estimation, the bending effect is equally important or even more important than tension. Thereby the stress contribution of bending cannot be ignored in the analysis.

It is easy to imagine the deformation process of the SG or ST's under tension load. At the beginning, a remarkable change of angles between arms occurs mainly due to bending, and the stiffness of the structure is low; as the tension load increases, the arms start stretching, which results in strong stiffness hardening. The process has been proved by finite element simulation using the shell model [6]. Bending and stretching are confirmed to act together throughout the deformation process.

3.2. Uniaxial tension analysis of super structures

In figure 1(b), the lengths along the x-axis and the y-axis of the Y-branched junction are $l_x = \sqrt{3}l$ and $l_y = 3l/2$. The elongations along the two directions are

$$\Delta l_x = \frac{\sqrt{3}Pl}{12E\pi D^2 \beta}(3 - 2\alpha^2)$$
$$\Delta l_y = \frac{Pl}{8E\pi D^2 \beta}(9 + 2\alpha^2). \quad (10)$$

So that the equivalent strains are calculated as

$$\varepsilon_x = \frac{\Delta l_x}{l_x} = \frac{P}{12E\pi D^2 \beta}(3 - 2\alpha^2)$$
$$\varepsilon_y = \frac{\Delta l_y}{l_y} = \frac{P}{12E\pi D^2 \beta}(9 + 2\alpha^2). \quad (11)$$

Therefore, the equivalent Poisson's ratio is

$$\tilde{\nu} = -\frac{\varepsilon_x}{\varepsilon_y} = \frac{2\alpha^2 - 3}{2\alpha^2 + 9}. \quad (12)$$

Equation (12) shows that the Poisson's ratio of SG or STs only depends on the slenderness ratio of arms, α. The equivalent tensional rigidity of a representative cell is obtained as

$$\tilde{k}_{cy} = \frac{P}{\Delta l_y} = \frac{8\pi E\beta D}{\alpha(9 + 2\alpha^2)}. \quad (13)$$

SG with the size $L_x \times L_y$ can be constructed by repeating the Y-branched structure in its plane, as shown in figure 1(a), m times along the x-axis and n times along the y-axis. The net structure can be considered as a plate with the equivalent thickness $\tilde{t}$, equivalent Young's modulus $\tilde{E}$ and Poisson's ratio

$\tilde{\nu}$. Wrapping the SG with the y-direction as the axis, a higher-order zigzag ST is obtained. According to the equivalence of the ST's circumference and the SG's width, the equivalent diameter of the ST is calculated from $\tilde{D} = L_x/\pi = m\sqrt{3}l/\pi$. The slenderness ratio and thickness ratio of the ST are defined as $\tilde{\alpha} = \tilde{l}/\tilde{D} = nl_y/\tilde{D}$ and $\tilde{\beta} = \tilde{t}/\tilde{D}$, respectively.

The slight change of angles between arms due to wrapping can be ignored except for STs with very small diameters. For simplicity, the results obtained based on SG are extended to STs. Therefore, the total deformation along the length direction is $\Delta L_y = n\Delta l_y = \frac{nP\alpha}{8\pi E\beta D}(9 + 2\alpha^2)$, and the tensional rigidity of the tube is

$$\tilde{k}_y = \frac{mP}{\Delta L_y} = \frac{8m\pi E\beta D}{n\alpha(9 + 2\alpha^2)}. \quad (14)$$

The axial rigidity of the ST is defined as

$$\tilde{E}\tilde{A} = \frac{\tilde{k}_y}{nl_y} = \frac{12m\pi E\beta D^2}{9 + 2\alpha^2}, \quad (15)$$

where $\tilde{A}$ is the equivalent cross-section area of the super tube. By adopting the expression of the arms' area, $A = \pi D^2 \beta$, the ratio of axial rigidity between the ST and m arms is

$$\frac{\tilde{E}\tilde{A}}{mEA} = \frac{12}{9 + 2\alpha^2}. \quad (16)$$

The ST is supposed as a hollow cylinder and its cross-section area is $\tilde{A} = \pi\tilde{D}\tilde{t} = \pi\tilde{D}^2\tilde{\beta}$. Thus equation (15) can also be derived as

$$\frac{\tilde{E}\tilde{\beta}}{E\beta} = \frac{4\pi^2}{m\alpha^2(9 + 2\alpha^2)}, \quad (17)$$

which is defined as the ratio of equivalent modulus.

In equation (17), the thickness ratio β is used to express the material parameter of a super tube by those of arm tubes. Generally, in finite element simulation of SWNTs by the shell model, the commonly used thickness and elastic modulus are obtained from the molecular dynamics method [13]. The equivalent thickness of 0.066 nm is quite different from the graphite interplanar spacing of 0.34 nm, and even smaller than the diameter of a carbon atom. Actually, it is hard and unnecessary to define a proper thickness of the single-atom sheet or super tube net, that is suitable for both tension and bending stiffness. From equations (5) and (6), we know that the axial tension stiffness EA and bending stiffness EI both linearly rely on β. This means that instead of Young's modulus E, an equivalent modulus $E\beta$ could be adopted to describe the modulus of a nanotube or super tube. The advantage of this equivalent modulus $E\beta$ is that, it is no longer necessary to separate the Young's modulus and thickness in stiffness calculations. In addition, the ratio of equivalent density can be obtained in terms of the equivalence of mass, expressed as $\tilde{\rho}\tilde{\beta}/(\rho\beta) = 2\pi^2/(3m\alpha^2)$. If the parameters of conductance and heat transmission also depend on the thickness of the nanotube, the thickness ratio β may be widely used instead of the thickness.

If $m = 10$ and $\alpha = 5$, then $\tilde{\nu} = 0.8$, $\tilde{E}\tilde{A}/(mEA) = 0.2$, and $\tilde{E}\tilde{\beta}/(E\beta) = 0.0027$ according to equations (12), (16) and (17). The results indicate that there is great shrinking in the radial direction for STs with slender arms, which results

Table 1. The results of equivalent tensional rigidity ($\frac{\tilde{E}\tilde{A}}{m}$) and Poisson's ($\tilde{v}$) ratio for SGs. Subscripts T and N mean theoretical analysis and numerical simulation. 'Error' denotes the relative error between the numerical and theoretical results.

Beam	α	β	$(\frac{\tilde{E}\tilde{A}}{m})_{\text{T}}$	$(\frac{\tilde{E}\tilde{A}}{m})_{\text{N}}$	Error (%)	$\tilde{v}_{\text{T}}$	$\tilde{v}_{\text{N}}$	Error (%)
Timo	5	0.033	463.9	370.5	20.1	0.797	0.838	5.2
Timo	8	0.053	122.0	109.9	9.9	0.913	0.926	1.4
Euler	5	0.033	463.9	452.7	2.5	0.797	0.802	0.6
Euler	8	0.053	122.0	119.0	2.5	0.913	0.920	0.8
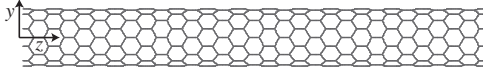
Figure 2. The scheme of a zigzag super tube.

Figure 3. (a) Equivalent tensional rigidity and (b) Poisson's ratio changing with α for STs with $m = 10$.

in the significant decrease of the STs' tensional rigidity and modulus compared with those of arm tubes. From the results of macroscopic mechanical analysis [11], Poisson's ratio is equal to 1.0 for regular-hexagonal honeycomb structures with solid rectangular sectional beams. It can be seen that the effect of angular rigidity of arms with annular sections is stronger than of those with solid sections. The value of Poisson's ratio depends on the slenderness ratio of the arms, known from equation (12). Thus the effect of angular stiffness will increase with the decrease of the slenderness ratio. It had been concluded in previous work [6] that, in small deformation, the SG structure is flexible, while in a finite deformation range, the hardening effect results in high rigidity. However, the material parameter expressions in the theoretical analysis here are limited to small deformation only.

3.3. Numerical simulation for uniaxial tension

In the above theoretical analysis, the Euler beam model is adopted. The Euler beam model ignores the shear deformation, which is only appropriate for slender arms. If the arms are not slender, the Timoshenko beam model should be used to incorporate the transverse shear deformation. In table 1, the numerical results obtained by Euler and Timoshenko (Timo) beams are compared with the theoretical predictions. In the simulation, super graphite with 20 cells in the width direction, $m = 20$, is subjected to a uniaxial tension strain of $\varepsilon_y = 0.005$. The arms of super graphite are two types of nanotube, SWNTs (15, 15) and (9, 9), with diameters of $D = 2.0$ and 1.24 nm, respectively. The thickness of SWNTs is $t = 0.066$ nm [13] and the arm length is $l = 10$ nm. The other parameters of the SWNTs come from the shell model [13]. As shown in table 1, the numerical results from the Euler beam model are quite close to theoretical predictions, while those from the Timoshenko (Timo) beam are slightly weaker due to the shear effect. It is clear that the discrepancy decreases with the increase of α.

As shown in figure 2, STs can be wrapped from SG, taking the zigzag type for example. Under uniaxial tension, a serials of STs with arms of different slenderness ratio α are examined. The thickness ratio β is kept constant for the same type of arm. In figure 3, the variation of equivalent tensional rigidity and Poisson's ratio with slenderness ratio α are drawn for super tubes with $m = 10$. The difference between the theoretical and numerical results is quite small. It can be concluded that the
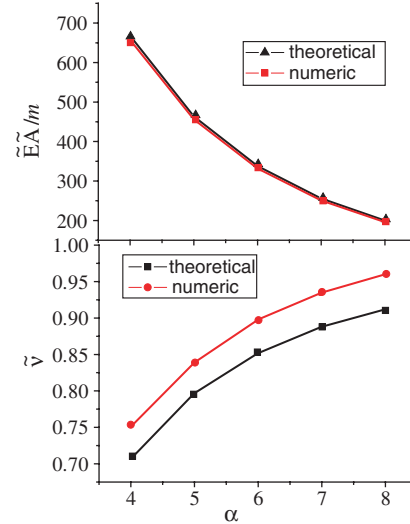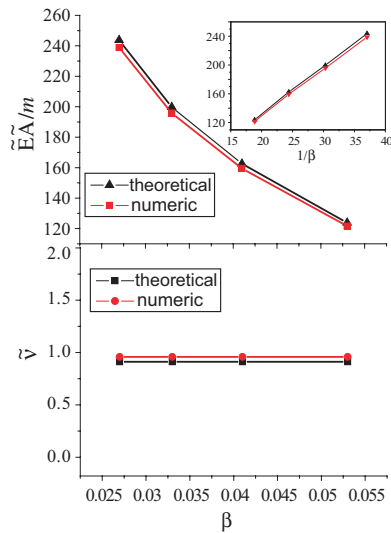
wrapping process from SG to STs has no obvious effect on the equivalent material parameters. The equivalent Poisson's ratios of super tubes are very high, close to 1, which means that the STs have great flexibility at the small deformation scale due to the angle change between arms. As the slenderness ratio α increases, the equivalent rigidity decreases, while Poisson's ratio has a tendency to increase.

The influence of the thickness ratio β on the tensional rigidity and Poisson's ratio is investigated by examining different STs with arms of SWNTs (18, 18), (15, 15), (12, 12) and (9, 9), respectively. Keeping the slenderness ratio α as a constant, the corresponding results of STs with different thickness ratio β are shown in figure 4. As predicted by equation (12), β almost has no effect on the equivalent Poisson's ratio for the super tubes. As regards the axial tensional rigidity, there is the relationship of $\tilde{E}\tilde{A} = (\frac{12m\pi Et^2}{9+2\alpha^2})\frac{1}{\beta}$, which is derived from equation (15) by substituting t/β for D. The curves of equivalent rigidity in figure 4 have exhibited this relationship, $\tilde{E}\tilde{A}$ linearly relying on $1/\beta$.

4. Bending analysis of a super tube

A super tube wrapped from super graphite is still supposed to be a hollow cylindrical tube with thin thickness. For a thin thickness ST, $\tilde{\beta} \ll 1$, the bending rigidity can be estimated as

$$\frac{\tilde{E}\tilde{I}}{\tilde{E}\tilde{A}} = \frac{\pi \tilde{D}^4 \tilde{\beta}(1 + \tilde{\beta}^2)/8}{\pi \tilde{D}^2 \tilde{\beta}} = \frac{1}{8}\tilde{D}^2(1 + \tilde{\beta}^2) \approx \frac{1}{8}\tilde{D}^2. \quad (18)$$

Figure 4. (a) Equivalent tensional rigidity and (b) Poisson's ratio changing with β for STs with $m = 10$.

**Table 2.** The numerical results for $\lambda = (\frac{\tilde{E}\tilde{I}}{\tilde{E}\tilde{A}})/(\frac{\tilde{D}^2}{8})$.

Load type	Beam type	λ	Beam type	λ
(a)	Timo	1.005	Euler	0.969
(b)	Timo	1.005	Euler	0.952
(c)	Timo	0.998	Euler	0.963

From equation (18), the bending rigidity of an ST is given without knowing the exact value of the tube thickness. It can be concluded that for a thin thickness super tube, $\tilde{\beta} \ll 1$, the bending stiffness $\tilde{E}\tilde{I}$ could easily be estimated from the axial tension stiffness $\tilde{E}\tilde{A}$, through simply multiplying by the parameter $\tilde{D}^2/8$.

The accuracy of equation (18) is validated by finite element simulation. A first-order zigzag super tube with arms of SWNT (15,15) is examined by numerical simulation. In the wrapping process, $m = 10$, $n = 30$, and the length of arms is $l = 10$ nm; thus the diameter and length of the ST are $\tilde{D} = 55.13$ nm and $\tilde{l} = 900$ nm. For a clamped super tube, with all the node degrees fixed on the clamped end, three types of loading are applied, respectively: (a) apply displacement load on the free end; (b) apply force on each node of the free end; (c) apply force on the up-surface nodes along a straight line parallel to the tube's axis. Having obtained the corresponding responses of the ST under each type of loading, the equivalent bending rigidity $\tilde{E}\tilde{I}$ can be calculated by using the formulae for a cantilever beam[1]. The axial tension stiffness $\tilde{E}\tilde{A}$ has been obtained in above section. Therefore, the parameter $\lambda = (\frac{\tilde{E}\tilde{I}}{\tilde{E}\tilde{A}})/(\frac{\tilde{D}^2}{8})$ is calculated, as shown in table 2.

The results indicated that $(\frac{\tilde{E}\tilde{I}}{\tilde{E}\tilde{A}})/(\frac{\tilde{D}^2}{8}) \approx 1$, which means that $\tilde{\beta}^2 \approx 0$ is confirmed by finite element simulations. The

---

[1] In Euler beam theory, there are three widely used formulae relating the deflection w and the bending rigidity EI for a cantilever beam with length l: $w = -Pl^3/(3EI)$ when a concentrated force P is applied on the free end; $w = -Ml^2/(2EI)$ when a flexural torque M is applied on the free end; and $w = -ql^4/(8EI)$ when a uniformly distributed load q is applied along the beam.
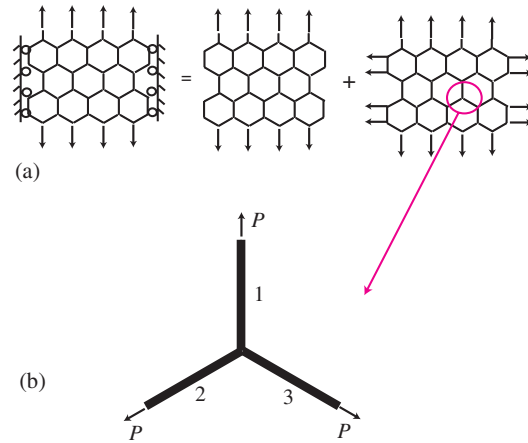
Figure 5. (a) Super graphite with no shrinking, (b) the force diagram of a Y-branched junction when the SG is subject to biaxial tension.

network structures of STs can be considered as thin hollow cylinders as long as the arms are slender enough.

Compared with a super tube, super graphite acts as a membrane, generally subject to in-plane tensile load. The bending rigidity of super graphite will be very low, thus no detailed discussion of its bending stiffness will be processed here.

5. Super tube with filling materials

From lower-order STs to higher-order STs, the reduction of stiffness and modulus are significant according to equations (16) and (17). Theoretical analysis and the finite element calculation tell us that stiffness reduction is caused by great radial shrinking of STs. If the shrinking could be suppressed, the deformation of STs will be greatly decreased. To achieve this modification, composite material needs to be considered. Suppose that STs are filled with matrix material having high bulk modulus, then the shrinking resistance will be significantly increased due to the inner support provided by the matrix. Thus a composite made up of super carbon nanotubes and high compressive rigidity matrix will have very good load-carrying capability.

Consider an extreme case of super graphite: there is no shrinking in the width direction. This stress condition is the superposition of two stress situations: uniaxial tension and biaxial tension, as shown in figure 5(a). Because of the great shrinking in an empty super tube, the biaxial tension loading condition will be the majority condition. The force diagram of a Y-branched junction in the biaxial tension case is shown in figure 5(b). In this case, each arm of the structure is under tension force P only, without any bending effect. The maximum total stress in the super graphite is just the tensile stress given by equation (8); there is no bending stress contribution expressed in equation (9). From the analysis in section 3.1, the bending stress is generally higher than tensile stress; thus the maximum total stress in the SG is remarkably reduced. The reduction of maximum stress will greatly increase the final strength of super graphite.

Besides the increase of strength, the stiffness will also be increased under the equal biaxial tension loading condition. The equivalent rigidity and modulus are obtained through

equilibrium analysis in a similar way to that above, and expressed as

$$\frac{\tilde{E}\tilde{A}}{mEA} = 1,$$

$$(19)$$

and

$$\frac{\tilde{E}\tilde{\beta}}{E\beta} = \frac{\pi^2}{3m\alpha^2}.$$

$$(20)$$

Comparing equations (19) and (20) with equations (16) and (17) for unfilled STs, the rigidity of the biaxial loading case will be strengthened greatly. Although the stiffness of the SG/ST is low, it will be improved by matrix material. Consequently, the mechanical properties of the ST composite are not the simple sum of the super tube and the filling materials. It will be improved by the interaction between ST/SG and matrix. As we know, a composite made up of CNTs and matrix is not as strong as expected, since CNTs always act as defects instead of reinforcement. A composite made of a regular network of ST/SG and matrix is predicted to have positive potential applications.

6. Conclusion

In summary, the equivalent mechanical properties of high-order super tubes are derived from the parameters of the low-order ones, in which each arm of the super tube is assumed to be a slender Euler beam. This derivation is applicable for any order of super tubes. The super tubes are assumed to be hollow cylinders with a thin thickness wall; thus a new equivalent modulus $E\beta$ instead of Young's modulus E is defined for the tubes. The advantage of this equivalent modulus is that the Young's modulus and thickness do not need to be separated in stiffness calculations. The analytical results are verified by finite element simulations. Under the slender beam assumption, the effect of stretching and bending are equally important for super tube deformation. Although the stiffness of super graphite and super tubes is low, it will be improved

by matrix material. Composites made of ST/SG and matrix are predicted to have high load-carrying capability.

References

[1] Li W Z, Wen J G and Ren Z F 2001 *Appl. Phys. Lett.* **79** 1879–81
[2] Biró L P, Ehlich R, Osaáth Z, Koós A, Horváth Z E, Gyulai J and Nagy J B 2002 *Diamond Relat. Mater.* **11** 1081–5
[3] Yin Y J, Chen Y L, Yin J and Huang K Z 2006 *Nanotechnology* **17** 4941–5
[4] Coluci V R, Galcao D S and Jorio A 2006 *Nanotechnology* **17** 617–21
[5] Dresselhaus M S, Dresselhaus G and Avouris P 2001 *Carbon Nanotubes Synthesis, Structure, Properties, and Applications* (Berlin: Springer)
[6] Wang M, Qiu X M and Zhang X 2007 *Nanotechnology* **18** 075711–6
[7] Shi J L, Hua Z L and Zhang L X 2004 *J. Mater. Chem.* **14** 795–806
[8] Meng G W, Jung Y J, Cao A, Vajtai R and Ajayan P M 2005 *Proc. Natl Acad. Sci.* **102** 7074–8
[9] Pugno N M 2006 *Nanotechnology* **17** 5480–4
[10] Li C Y and Chou T W 2003 *Int. J. Solids Struct.* **40** 2487–99
[11] Gibson L J and Ashby M F 1997 *Cellular Solids: Structure and Properties* (Cambridge: Cambridge University Press)
[12] Onck P R, Andrews E W and Gibson L J 2001 *Int. J. Mech. Sci.* **43** 681–99
[13] Yakobson B I, Brabec C J and Bernholc J 1996 *Phys. Rev. Lett.* **76** 2511–4